Assessment of Run-Up Height and Arrival Time of 365 AD Tsunami at Lampedusa Island, Italy

FX Anjar Tri Laksono[1,2*], *Manoranjan* Mishra[3], and *Kovács* János[1]

[1]University of Pécs, Department of Geology and Meteorology, 7624 Pécs, Hungary
[2]Jenderal Soedirman University, Geological Engineering Department, 53371 Purbalingga, Indonesia
[3]Fakir Mohan University, Geography Department, 756020 Odisha, India

Abstract. The eastern Mediterranean Sea is a subduction zone between the African plate and the Eurasian plate that has high seismicity. The tsunami of July 21, 365 AD was one of the most severe in the region, and its impact was estimated to have extended to the islands around the Aegean Sea, Cyprus, southern Calabria, Sicily, Malta, and Lampedusa. However, an analysis of tsunami waves reaching Lampedusa Island has not been conducted. Therefore, this study will present the run-up height and arrival time of tsunami waves near the Lampedusa coast. The methods applied are linear and non-linear shallow water equations by inputting the rupture parameters of the 365 AD earthquake. We used Delft Dashboard and Delft3D software to simulate tsunami wave propagation offshore. The simulation results indicate that an earthquake with a magnitude of approximately Mw 8.5 triggered tsunami waves with a maximum run-up height of 2.02 m in nearshore Lampedusa. The travel time for the maximum run-up height was 3.5 hours after the generation of the first tsunami wave in the western Hellenic Arc, Greece. We infer that seawater most likely inundated the coast of Lampedusa during the tsunami earthquake in 365 AD.

1 Introduction

The Mediterranean Sea hosts two subduction systems, the Hellenic and Calabrian Arcs, which exhibit high seismicity [1,2]. The Hellenic Arc once generated an M_w>8 earthquake, followed by tsunami waves, on 21 July 365 AD [3–5]. Meanwhile, the Calabrian Arc has recorded several Mw = 7 tsunamigenic earthquake, which induced the deposition of Late Quaternary turbidites in the deep basin [6,7]. To date, the 365 AD tsunami is recorded as the largest tsunami event in the Mediterranean Sea due to its extensive destruction spanning Greece, Egypt, Libya, Tunisia, Algeria, Palestine, Cyprus, Calabria, the east coast of Sicily, and western Anatolia [8–12]. This statement is supported by the discovery of tsunami deposits in Crete, Augusta, Messina, Ognina, Catania, and Syracuse, which were dated to correspond with the 365 AD tsunami [8,10,11,13–17]. However, identical deposits were not found in southern Sicily or the surrounding islands. Furthermore, there has been no research on tsunami wave modeling in southern Sicily or the surrounding islands, which could be useful in determining the furthest extent of tsunami wave propagation westwards from the Hellenic Arc and finding evidence of tsunami deposits in the region. A rupture modeling study of the 365 AD earthquake conducted by Ohsumi et al. [18] and Papadimitriou & Karakostas [19] suggests that the magnitude of the earthquake might have reached Mw 8.4. On the other hand, Ambraseys [20] and Hamouda [21] suggested that the magnitude of this earthquake could be even higher, up to Mw 8.5. This research aims to present the possible run-up height and arrival time of the 365 AD tsunami waves on Lampedusa Island (Fig. 1), using the worst-case earthquake magnitude scenario of Mw 8.5. Lampedusa Island was chosen because it is located approximately 300 km southwest of Sicily and 150 km east of Tunisia, where tsunami deposits related to the 365 AD tsunamigenic earthquake have not yet been found. The assessment of the tsunami at Lampedusa aims to evaluate the likely maximum distance that the tsunami waves could reach.

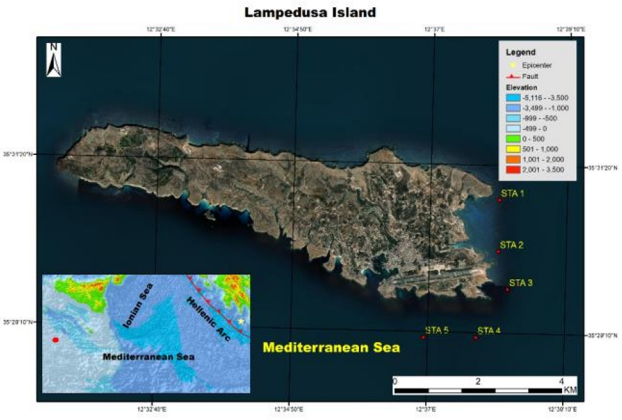

Fig. 1. Lampedusa Island is situated in the Mediterranean Sea, roughly 850 km from the epicenter of the 365 AD tsunamigenic earthquake in the western Hellenic Arc, Greece.

* Corresponding author: anjar93@gamma.ttk.pte.hu

2 Methodology

We adopted the earthquake rupture parameters (Table 1) of the worst-case tsunamigenic earthquake scenario that occurred in 365 AD with a magnitude of Mw = 8.5 [21–24]. The epicenter of this earthquake is located along the western Hellenic Arc, approximately 850 km to the east of Lampedusa Island (Fig. 2) [18,19,21]. The fault displacement length required to generate an earthquake of this magnitude in this area is 365 km. For the simulation of tsunami wave generation and propagation from the earthquake source, we employed the shallow water equation [25,26]. The linear shallow water equation was implemented to describe tsunami wave propagation offshore (depth >50 m), while the non-linear shallow water equation was utilized to simulate tsunami waves reaching the nearshore (depths between 2 m and 50 m). The principle behind this option is related to the fact that the wavelength offshore is relatively longer compared to the waves in the nearshore, while the wave height offshore is lower than that of the tsunami waves when they arrive in the nearshore [27–29].

Table 1. Fault displacement parameters of the 365 AD tsunamigenic earthquake used in the simulation of tsunami wave generation and propagation.

Fault parameter	Rupture input
Strike (º)	~N113E-N147E
Dip (º)	35
Length (km)	365
Width (km)	80
Rake (º)	90
Slip (m)	25
Depth (km)	5

Numerical modeling of tsunami wave propagation from the earthquake source to the nearshore of Lampedusa Island was conducted by integrating Delft Dashboard and Delft3D software using a rectangular grid with a resolution of 10 km. The Riemann boundary type was selected to ensure that tsunami waves reaching Lampedusa Island would be reflected back towards the initial point of generation, allowing for the observation of overwash and backwash processes [27,28]. There are five observation points in the nearshore of Lampedusa (Fig. 1) where water level and tsunami wave arrival time were measured. The bathymetry of each observation location is provided in Table 2. The bathymetry data used was sourced from Gebco 19.

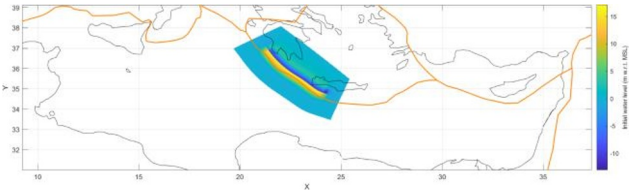

Fig. 2. illustrates the fault displacement area, which served as the source of the earthquake and tsunami that occurred in 365 AD. This fault displacement area was utilized to simulate the initial generation of tsunami waves, which propagated towards the nearshore of Lampedusa Island, located in southwestern Sicily, Italy.

Table 2. Coordinate location and depth of observation points for measuring the run-up height and arrival time of tsunami wave propagation in the nearshore of Lampedusa.

Observation	Latitude	Longitude	Depth (m)
STA 1	35.5151	12.6318	13
STA 2	35.5049	12.6319	9
STA 3	35.4952	12.6370	32
STA 4	35.4853	12.6274	49
STA 5	35.4850	12.4220	50

3 Results and discussion

The simulation results at STA 1 indicate that at the 130th minute after the generation of the first tsunami wave in the western Hellenic Arc, the water level reached 0.5 m. It then increased to 1.1 m within 10 minutes (Fig. 3 A). However, after 2.5 hours from the generation of the first wave from the earthquake source, the water level at STA 1 decreased to 0.85 m. Within 50 minutes, the run-up height at this location is only 0.34 m. The wave height rose again significantly to 1.46 m at the 210th minute after the generation of the first wave (Fig. 3 A and Fig. 4 A, B, C, D, E, and F). In the following minutes, the water level declined until it returns to the normal wave height. At STA 2, the water level rose to 0.46 m after 130 minutes of the tsunami hitting the western Hellenic Arc. The run-up height reached a peak of 1.5 m at the 140th minute and then continued to drop to only 0.07 m at the 180th minute or 3 hours after the first wave appeared at the source (Fig. 3 B). At 190 minutes, the water level increased to 0.6 m, and within 20 minutes, the run-up height reached 2.02 m before dropping to 0.6 m 30 minutes later. At STA 3, a water level rise of 0.39 m occurred after 130 minutes of tsunami wave generation. Similar to STA 1 and STA 2, at the 140th minute, the run-up height attained a maximum of 1.39 m and then declines to 1.25 m and 0.63 m at the 150th and 180th minutes, respectively (Fig. 3 C). The water level rose again to 1.45 m 30 minutes later and then decreased

in the following minutes. At STA 4, the water level slowly rose from 0 m at the 120th minute to 0.06 m at the 130th minute (Fig. 3 D). The maximum run-up height of 0.64 m is achieved after 140 minutes of the first wave generation (Fig. 3 D and Fig. 4 E). Subsequently, the water level dropped to 0.01 m at the 160th minute before finally rising again to reach the second maximum run-up height of 1.3 m at the 190th minute. At STA 5, there was also an increase in the water level from 0 m to 0.1 m at the 120th and 130th minutes (Fig. 3 E). The first maximum run-up height of 0.75 m took place after 2.5 hours of the first tsunami wave generation. The second maximum run-up height of 1.9 m was observed at the 220th minute or approximately 3.5 hours after the generation of tsunami waves in the western Hellenic Arc (Fig. 3 E and Fig. 4 F).

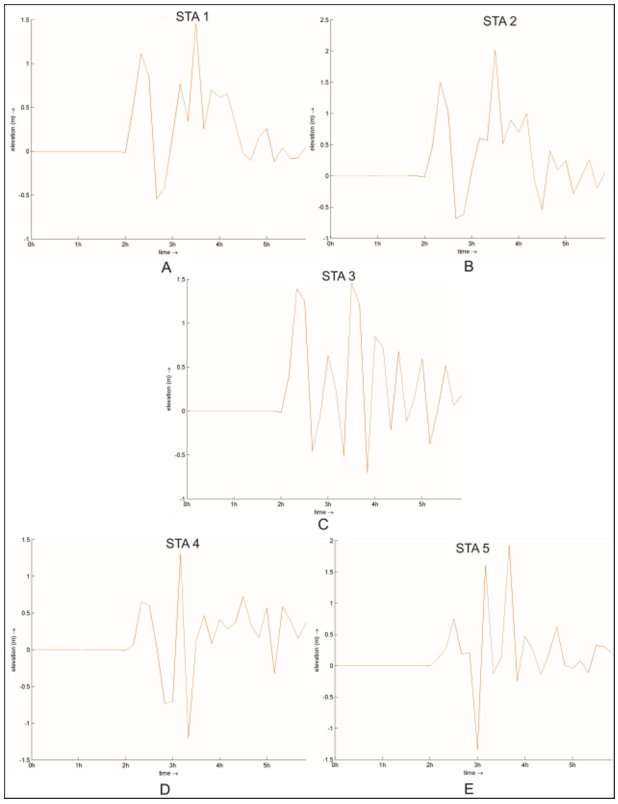

Fig. 3. Diagram of the relationship between the height and arrival time of tsunami waves at A. STA 1, B. STA 2, C. STA 3, D. STA 4, E. STA 5. The propagation time and water level of the tsunami waves at each observation location are similar, with the arrival time at the 130th minute and the maximum run-up height occurring 2.5 hours and 3.5 hours after the generation of the first tsunami wave in the western Hellenic Arc.

The analysis of the travel time and run-up height of the tsunami waves reveals a similar arrival time of 2 hours and 10 minutes after the generation of the first tsunami wave in the Western Hellenic Arc. Additionally, at each observation location, there are two phases of tsunami run-up, with the first phase occurring at the 150th minute and the second run-up phase taking place at the 210th minute. Generally, the water level in the second run-up phase is higher than that in the first run-up phase. During the interval between the first and second run-up phases, the water level decreases significantly. Table 3 presents important information on the arrival time and maximum run-up height in the first and second run-up phases at each observation location.

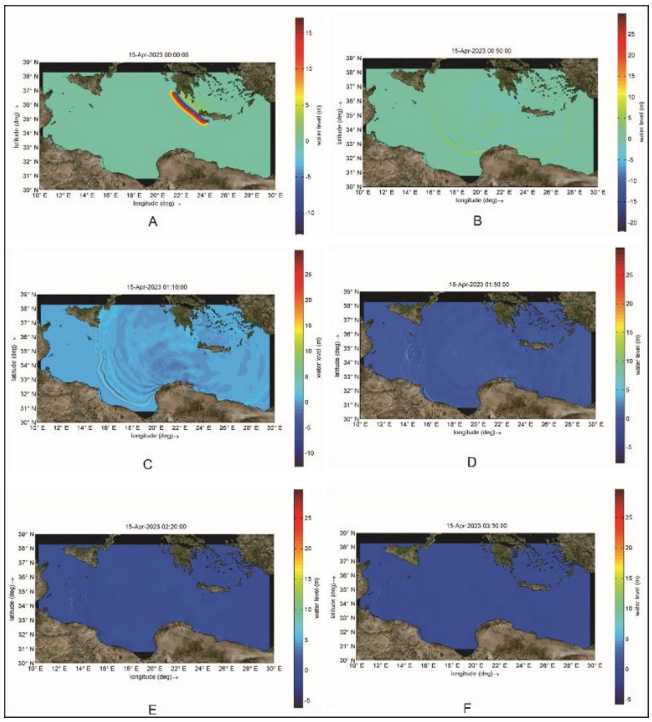

Fig. 4. The tsunami waves propagation process from the Western Hellenic Arc traveled westwards towards Lampedusa Island. Each figure represents the wave propagation at minutes A. 0, B. 50, C. 70, D. 110, E. 140, and F. 210. The tsunami waves reached the eastern coast of Sicily about one hour after the generation of the tsunami waves. Within 2 hours and 20 minutes, the tsunami waves arrived at Lampedusa Island.

Table 3. Arrival time and maximum run-up height at each observation location. The maximum run-up height at STA 2 measured 2.02 m, which occurred 210 minutes after the initial generation of tsunami waves.

Location	First max run-up time (minute)	First max run-up height (m)	Second max run-up time (minute)	Second max run-up height (m)
STA 1	140	1.1	210	1.46
STA 2	140	1.5	210	2.02
STA 3	140	1.39	210	1.45
STA 4	140	0.64	190	1.3
STA 5	150	0.75	220	1.9

The simulation of the 365 AD tsunami wave propagation in Lampedusa reinforces previous research that stated the impact of the 365 AD tsunami could reach Tunisia and Libya [10,12,30,31]. Tunisia is geographically located west of Lampedusa and farther from the epicenter of the 365 AD earthquake in the

Western Hellenic Arc than the distance between the western Hellenic Arc and Lampedusa. At Ghar El Meleh, sediments of the 365 AD tsunami have been found, with an estimated maximum run-up height of more than 1 m. Bahrouni et al. [12] estimated a higher run-up height of up to 3.5 m. This estimation was derived from numerical modeling of tsunamis generated by earthquakes in the western Hellenic Arc. However, this interpretation was not supported by evidence of tsunami deposits in northeastern Tunisia. Therefore, considering that the wave propagation of the 365 AD tsunami extended to the east coast of Tunisia and the north coast of Libya, the 365 AD tsunami simulation, which suggests that the maximum run-up height at Lampedusa exceeded 1 m, is reliable. However, a definitive forecast of the maximum run-up height at Lampedusa requires support from evidence of tsunami deposits, as conducted by Kohila et al. [31] in northeastern Tunisia.

The run-up height of tsunami waves is strongly influenced by factors such as earthquake magnitude and distance from the earthquake source [32,33]. Meanwhile, earthquake magnitude is closely related to rupture parameters of fault displacement, such as fault length, fault width, depth, rake, strike, dip, and slip [34]. The longer and wider the fault, the greater the earthquake magnitude and the higher the water level [35]. In the case of the 365 AD tsunami in the western Hellenic Arc, Greece, the minimum length and width of fault displacement required to generate an Mw 8.5 earthquake were 350 km and 80 km, respectively. This criterion differs from the statement of Papadimitriou and Karakostas [19], who estimated a fault displacement length of 160 km to generate an Mw 8.3 earthquakes. The distance of the observation location from the earthquake source will affect the arrival time of tsunami waves. The farther a location is from the initial generation of tsunami waves, the longer the arrival time will be, and the waves will also experience a reduction in amplitude and propagation rate [36,37].

The accuracy of tsunami wave simulations is highly dependent on various factors, including the resolution of bathymetry, grid resolution, grid type, and input parameters such as fault rupture, water density, roughness, wind, and gravity [38,39]. Simulations with higher bathymetry and grid resolution tend to produce more accurate results compared to lower resolutions [40,41]. Additionally, gravity plays a crucial role in tsunami wave simulation. In the case of the Sunda Strait tsunami, it is likely that the strong lunar gravity at the time of the event contributed to significant wave heights when the tsunami reached the coastline of Anyer, Banten, Indonesia [42,43]. However, in other tsunami events such as the Tohoku tsunami in Japan in 2011 and the Indian Ocean tsunami in 2004, lunar gravity did not have a prominent influence on the generation and propagation of tsunami waves to land [44,45]. When referring to the 365 AD tsunami wave simulations conducted by Ohsumi et al. [18], Hamouda [21], Ambraseys [46], Papadimitriou and Karakostas [19], the influence of the moon's gravity is considered negligible, and therefore, the gravity parameter adopted is the earth's gravity of 9.81 m/s².

4 Conclusions

The tsunami waves that occurred in 365 AD in the western Hellenic Arc could possibly reach Lampedusa Island within 130 minutes after the initial wave generation. The maximum run-up height at the five observation sites varied from 1.3 m to 2.02 m with a tendency for the water level in the second phase of run-up to be higher than that in the first phase of run-up. The maximum run-up height in the first phase of run-up occurred in the 140^{th} to 150^{th} minutes while in the second phase of run-up, it took place in the 190^{th} to 220^{th} minutes. The results of this simulation can be used as a reference to search for evidence of tsunami deposits on Lampedusa Island, which has never been undertaken until now. Furthermore, the post-depositional process factor needs special attention in the search for paleotsunami deposits.

This research was funded by UNKP under research grant number UNKP-22-3-1. The publication of this article was financed by the University of Pécs, Hungary.

References

1. S. Tinti, A. Maramai, L. Graziani, Nat. Hazards **33**, 439 (2004)
2. A. Polonia, C.H. Nelson, S.C. Vaiani, E. Colizza, G. Gasparotto, G. Giorgetti, C. Bonetti, L. Gasperini, Sci. Rep. **12**, 5253 (2022)
3. B. Shaw, N.N. Ambraseys, P.C. England, M.A. Floyd, G.J. Gorman, T.F.G. Higham, J.A. Jackson, J.M. Nocquet, C.C. Pain, M.D. Piggott, Nat. Geosci. **1**, 268 (2008)
4. S.C. Stiros, Quat. Int. **216**, 1-2 (2010)
5. S. Lorito, M.M. Tiberti, R. Basili, A. Piatanesi, G. Valensise, J. Geophys. Res. Solid Earth **113**, B01301 (2008)
6. A. Polonia, C.H. Nelson, S. Romano, S.C. Vaiani, E. Colizza, G. Gasparotto, L. Gasperini, Mar. Geol. **384**, 177 (2017)
7. A. Polonia, E. Bonatti, A. Camerlenghi, R.G. Lucchi, G. Panieri, L. Gasperini, Sci. Rep. **3**, 1285 (2013)
8. V. Werner, K. Baika, P. Fischer, H. Hadler, L. Obrocki, T. Willershäuser, A. Tzigounaki, A. Tsigkou, K. Reicherter, I. Papanikolaou, K. Emde, A. Vött, Quat. Int. **473**, 66 (2018)
9. S.C. Stiros, J. Struct. Geol. **23**, 545 (2001)
10. A. Di Vita, Ann. Geophys. **38**, 971 (1995)
11. P.M. De Martini, M.S. Barbano, A. Smedile, F. Gerardi, D. Pantosti, P. Del Carlo, C. Pirrotta, Mar. Geol. **276**, 42 (2010)
12. N. Bahrouni, M. Meghraoui, H.B. Bayraktar, S.

Lorito, M.F. Zagrarni, A. Polonia, N. Bel Mabrouk, M. Kamoun, A. Khadraoui, F. Kamoun, EGU **22**, 9383 (2022)

13. A. Smedile, F. Molisso, C. Chagué, M. Iorio, P.M. De Martini, S. Pinzi, P.E.F. Collins, L. Sagnotti, D. Pantosti, Sedimentology **67**, 1553 (2020)
14. F. Gerardi, A. Smedile, C. Pirrotta, M.S. Barbano, P.M. De Martini, S. Pinzi, A.M. Gueli, G.M. Ristuccia, G. Stella, S.O. Troja, Nat. Hazards Earth Syst. Sci. **12**, 1185 (2012)
15. A. Smedile, P.M. De Martini, D. Pantosti, L. Bellucci, P. Del Carlo, L. Gasperini, C. Pirrotta, A. Polonia, E. Boschi, Mar. Geol. **281**, 1 (2011)
16. G. Scardino, A. Rizzo, V. De Santis, D. Kyriakoudi, A. Rovere, M. Vacchi, S. Torrisi, G. Scicchitano, Quat. Int. **638**, 122 (2021)
17. A. Scheffers, S. Scheffers, Earth Planet. Sci. Lett. **259**, 613 (2007)
18. T. Ohsumi, Y. Dohi. H. Hazarika, J. Disaster Res. **13**, 943 (2018)
19. E.E. Papadimitriou, V.G. Karakostas, Acta Geophys. **56**, 293 (2008)
20. N.N. Ambraseys, J. Seismol. **5**, 263 (2001)
21. A.Z. Hamouda, Acta Geophys. **58**, 687 (2010)
22. S. Yolsal-Çevikbilen, T. Taymaz, Tectonophysics **536**, 61 (2012)
23. R. Tonini, A. Armigliato, G. Pagnoni, F. Zaniboni, S. Tinti, Nat. Hazards Earth Syst. Sci. **11**, 1217 (2011)
24. B.L. Valle, N. Kalligeris, A.N. Findikakis, E.A. Okal, L. Melilla, C.E. Synolakis, Proc. Inst. Civ. Eng. Eng. Comput. Mech. **167**, 99 (2014)
25. R.A. Khan, N.K.R. Kevlahan, *Ocean Model.* **174**, 102009 (2022)
26. C. Sánchez-Linares, M. de la Asunción, M.J. Castro, S. Mishra, Šukys, J, Appl. Math. Model. **39**, 7211 (2015)
27. F.A.T. Laksono, M.R. Aditama, R. Setijadi, G. Ramadhan, IOP Conf. Ser. Mater. Sci. Eng. **982**, 012047 (2020)
28. F.A.T. Laksono, *Assessment of building vulnerability to tsunami using the PTVA-4 method: case study of the 2006 Cilacap tsunami tragedy* (Nova Science Publishers, New York, 2023)
29. F.A.T. Laksono, A. Widagdo, M.R. Aditama, M.R. Fauzan, J. Kovács, Sustain. **14**, 5 (2022)
30. N.N. Ambraseys, C.P. Melville, R.D. Adams, *The seismicity of Egypt, Arabia and the Red Sea* (Cambridge University Press, Cambridge, 1994)
31. B.S. Kohila, L. Dezileau, S. Boussetta, T. Melki, N. Kallel, Nat. Hazards Earth Syst. Sci. **21,** 3645 (2021)
32. D. Melgar, Y. Bock, J. Geophys. Res. Solid Earth **120**, 3324 (2015)
33. J.G.F. Crempien, A. Urrutia, R. Benavente, R. Cienfuegos, Sci. Rep. **10**, 8399 (2020)
34. C. Mueller, W. Power, S. Fraser, X. Wang, J. Geophys. Res. Solid Earth **120**, 488 (2015)
35. F. Løvholt, G. Pedersen, S. Bazin, D. Kühn, R.E. Bredesen, C. Harbitz, J. Geophys. Res. Ocean. **117**, 3 (2012)
36. S.N. Ward, J. Phys. Earth **28**, 5 (1980)
37. Ö. Necmioğlu, N.M. Özel, Oceanography **27**, 2 (2014)
38. D. Dutykh, R. Poncet, F. Dias, Eur. J. Mech. B/Fluids **30**, 6 (2011)
39. I.A. Williams, D.R. Fuhrman, Coast. Eng. **110**, 17-31 (2016)
40. V. Titov, F. Gonzalez, NOAA Tech. Memo. ERL PMEL-112 **1760**, 301 (1997)
41. M. Van Ormondt, K. Nederhoff, A. Van Dongeren, J. Hydroinformatics **22**, 3 (2020)
42. S.T. Grilli, D.R. Tappin, S. Carey, S.F.L. Watt, S.N. Ward, A.R. Grilli, S.L. Engwell, C. Zhang, J.T. Kirby, L. Schambach, M. Muin, Sci. Rep. **9**, 11946 (2019)
43. W. Widiyanto, S.C. Hsiao, W.B. Chen, P.B. Santoso, R.T. Imananta, W.C. Lian, Nat. Hazards Earth Syst. Sci. **20**, 4 (2020)
44. B.T. MacInnes, A.R. Gusman, R.J. LeVeque, Y. Tanioka, Bull. Seismol. Soc. Am. **103**, 2 (2013)
45. X. Wang, P.L.F Liu, J. Hydraul. Res. **44**, 2 (2006)
46. N. Ambraseys, *Earthquakes in the Mediterranean and Middle East: A multidisciplinary study of seismicity up to 1900* (UC Press, Berkeley, 2015)